International Journal of Computational and Experimental Science and Engineering (IJCESEN)
Vol. 4-No.3 (2018) pp. 43-50
http://dergipark.gov.tr/ijcesen

ISSN: 2149-9144

Research Article

Thermal Analysis of a Zirconium Dioxide Coated Aluminum Alloy Piston

Murat OZSOY[1]*, Ismet TIKIZ[2], Huseyin PEHLIVAN[1]

[1] Sakarya University, Engineering Faculty, Mechanical Engineering Department, Sakarya, TURKEY
[2] Kırklareli University, Engineering Faculty, Mechanical Engineering Department, Kırklareli, TURKEY

* **Corresponding Author** : ozsoy@sakarya.edu.tr
ORCID: 0000-0003-2400-5212

Article Info:

DOI: 10.22399/ijcesen.479222
Received : 06 November 2018
Accepted : 26 November 2018

Keywords

Thermal analysis
Finite element method
Thermal barrier coating
Aluminum alloy piston

Abstract:

Performance and operating costs are the most important factors in internal combustion engines. It is one of the most commonly used methods to coat pistons with advanced technological ceramic materials in order to improve performance and fatigue life in internal combustion engines. In this study, changes in temperature and heat flux were investigated in various thickness coatings made on a 2500 cc turbo diesel engine piston. As bonding coat, NiCrAl was used in a thickness of 0.2 mm, while ZrO_2 (zirconium dioxide) was used in thicknesses of 0.2-0.4-0.6 and 0.8 mm as thermal barrier coating material. The piston was modeled in PTC Creo parametric software and then transferred to ANSYS Workbench environment to create a mathematical model. Engineering calculations were also done using the finite element method. After the calculation, the temperatures at the depth of 5 mm from the combustion chamber upper surface, the binder layer upper surface, the thermal coating upper surface and the combustion chamber upper surface were compared. As a result, it was observed that the combustion chamber and the section at the depth of 5 mm from the combustion chamber had a temperature decrease of 13%.

1. Introduction

Thermal barrier coatings (TBCs) are extensively applied to protect metallic components of aircraft engines in an aggressive environment for improving the engine efficiency by increasing operating temperatures [1]. The zirconia based materials got increasing interest in the thermal barrier coatings [2]. These ceramic coatings help increase the entry temperature, which translates to higher performance and efficiency of the engine. However, with an ever-increasing demand for higher operating temperatures, a failure mode related to interaction between the ceramic coatings and molten deposits significantly affects the durability of TBCs [3]. Thermal barrier coatings (TBCs) have been widely used to provide thermal protection for the hot-section metal components in advanced gas turbines and diesel engines to improve thermal efficiency and performances [1–3]. Currently, 6–8 wt.% Y_2O_3 stabilized zirconia (YSZ) is considered as a good choice for the ceramic top coat material due to its superior durability during thermal cycling [4].

Ramaswamy at al. [5] study involves the need and developmental efforts made via Computational Fluid Dynamics (CFD) to generate a model via ANSYS - Fluent simulation software that predicts the temperature gradient across Thermal Barrier Coatings of different type ceramics and coating thicknesses.

To determine the optimum coating thickness, Dudavera at all. [6] simulated the thermal state of the piston using ANSYS Multiphysics. In this study, motor tests of the pistons using the single-cylinder unit of a four-cylinder two-stroke engine. The coating was applied to the surface of the piston head on the combustion chamber side.

Bolek at al. [7], investigate thermal barriers composed of ZrO_2 + 20%Y_2O_3 and β-NiAl intermetallic diffusion layers were fabricated on Inconel 713C. The numerical simulation of the real shape of the interface between the layers revealed

that stress concentration zones occur not only at the peaks and valleys of the interface but also on the semi-flat surface in the midway between them.

Kumar at al. [8] has researched material structural forms. The analysis was carried out for Al - ZrO_2 combination with different volume fraction indices. A parametric study with different power-law indices, thickness ratios, aspect ratios, support conditions and load parameters on non-dimensional centroidal deflection had been performed.

Yerrennagoudaru and Manjunatha [9] designed conventional and modified piston in the Unigraphics software and the resulting flow field was analyzed for different piston configurations by using CFD software Fluent ANSYS-14.5. Compere temperature in conventional piston and modified piston, during analysis conventional piston means without ceramic and platinum coating, modified piston means with without ceramic and platinum coating and for these pistons Swirl ratio, Tumble ratio Y, Cross Tumble Ratio graphs has drawn.

Ma at al. [10] was investigated ultrasonic vibration was introduced to assist laser clad coatings, and the effect of ultrasonic vibration on the cross section morphology, microstructure evolution and dilution characteristics between coating and substrate. Thermal and structure finite element analysis has been employed to be informed the thermal stresses developed in Al_2O_3-SG, ZrO_2-12%Si+Al and ZrO_2-SG coatings subjected to thermal loading by Kocabicak at all. [11]. Systems with 0.4 mm coating thickness and 4 mm substrate material thickness were modelled. The finite element technique can be used to optimise the design and the processing of ceramic coatings.

Celik ve Sarikaya [12] were investigated the effect on residual stresses of porosity in MgO–ZrO_2 coatings on Al–Si alloy substrate. Thermal loads were applied to the model at the temperature of 550^{o}C using finite element method. Finite element calculations demonstrated that the highest thermal shock resistance was reached in the coating system with 7.5% small size sphere shape and uniformly distributed porosity. The coating with above 7.5% porosity had maximum values in radial, axial and shear stresses.

Taymaz at al. [13] studies the effect of surface preparation techniques. Thermal and structural finite element analysis has been employed to analyse the level of stresses developed Al_2O_3–SG, ZrO_2 (12% Si+Al) and ZrO_2–SG coatings subjected to thermal loading. Nominal and shear stresses at the critical interface regions (film/interlayer/substrate) were obtained and compared. The results showed that the ZrO_2–SG coatings have a higher thermal shock resistance than the Al_2O_3–SG and ZrO_2 (12%Si+Al) coating systems.

Thermal analysis evolution of MgO–ZrO_2/NiCrAlY coatings on Ni metal and AlSi alloy (LM13) substrates was studied by Sarikaya and Celik [14]. MgO–ZrO_2/NiCrAlY coatings were deposited on metallic substrates using an atmospheric plasma spray technique. Thermal loadings were applied to the model at the temperature range 800–1000 °C using finite element method. It was also found that the larger residual stresses were obtained with an increase of the coating thickness and interlayer bond coatings decreased residual stresses.

Mimaroglu at al. [15] employed coupled (thermal and structure) finite-element analysis to analyse the influences of porosity volume, size and distribution in MgO.ZrO_2-GG coating subjected to thermal loading. The results showed that the volume, size, location and distribution of the porosity have a significant influence on the level of the developed thermal stresses in the case of MgO.ZrO_2-GG coatings the optimum low-level stresses are developed with 7% small-size uniformly-distributed porosity allocated far away from the coating surface.

Khor and Gu [16] prepared coatings with different thicknesses and coating layers for bond strength and thermal cycling resistance tests. They were studied the microstructure, micro hardness, density, elastic modulus, thermal conductivity/diffusivity and coefficient of thermal expansion. The 8 wt.% Y_2O_3 stabilized ZrO_2 and NiCoCrAlY powders were used for the FGM coatings. The thermal cycling life of five-layer FGM coating is five times higher than that of the duplex coating which can be indicated from the FEA results.

Finite element code in ANSYS has been employed to analysis fracture in ceramic coatings subjected to thermal loading by Mimaroglu at all. [17].

Hypothetical material properties have been considered as material data for coupled (thermal and structure) finite element analysis and evaluated the stress intensity factors in different coatings. The results showed that the shorter the crack length and the thinner the coating, the sounder the coatings. Furthermore, coatings representing a wide range of thermal and mechanical properties have a close normalized stress intensity factor values. It is also concluded that the finite element technique can be used to optimize the design and the processing of ceramic coatings

As a result of the literature review made above, there is an increasing number of experimental and numerical studies on the thermal analysis of pistons. Generally, although bond materials were the same, different types of coating materials were

used. In this study, the temperature distribution was examined for the original model and thermally coated model with four different thicknesses.

2. Geometric and Mathematical Modelling of the Piston

Geometric model of the piston body is modelled as a solid model at PTC Creo Parametric software. After modelling the piston body, first a 0.2 mm binding layer then thermal barrier coats with thicknesses of 0.2 mm-0.4 mm-0.6 mm and 0.8 mm modelled. Then for each thermal barrier coat a new assembly modelled, at last for finite element analyses four types of geometric models created. The Figure1 shows information about the properties of the geometric models.

H is a virtual path has 91 points on it for post processing. This path is created on the top surface of combustion chamber, 5 mm below the combustion chamber, on top surface of bond coat (binding layer) and on top surface of thermal coat.

After creating the geometric models of the original and thermal barrier coated pistons at PTC Creo Parametric, models were transferred to the Ansys Workbench software which is used for calculation by the finite element method. There are five types of models, first is original piston, second is 0.2 mm NiCrAl binding layer and 0.2 mm ZrO_2 thermal barrier coated, third is 0.2 mm NiCrAl binding layer and 0.4 mm ZrO_2 thermal barrier coated, fourth is 0.2 mm NiCrAl binding layer and 0.6 mm ZrO_2 thermal barrier coated and last one is 0.2 mm NiCrAl binding layer and 0.8 mm ZrO_2 thermal barrier coated.

After creating and transferring the geometric model to the ANSYS Workbench environment, the most important step is creating the mesh. For creating a healthy mesh, mesh metrics-element quality method was used. The Element quality option provides a composite quality metric that ranges between 0 and 1. This metric is based on the ratio of the volume to the sum of the square of the edge lengths for 2D quad/tri elements, or the square root of the cube of the sum of the square of the edge lengths for 3D elements. A value of 1 indicates a perfect cube or square while a value of 0 indicates that the element has a zero volume [18]. Table 1 shows the number of mesh, elements and also element quality of each mathematical model. All models have same bond coat as NiCrAl with a thickness of 0.2 mm so at table only thermal barrier coat included. Also a meshed model of one coated piston can be seen at Figure 2. During the meshing for binding layer and thermal barrier coat 0.1 mm element size of vertical direction used for a better mesh quality.

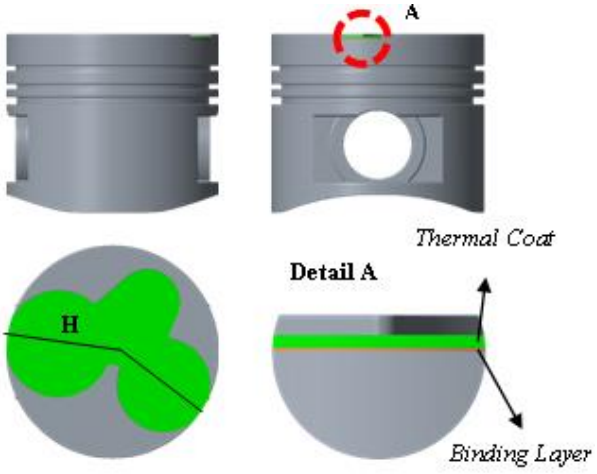

Figure 1. *Geometric model of the thermal coated piston.*

Table 1. *Mesh statics-element quality of original and thermal barrier coated pistons*

Model Properties	Mesh Statistics		Element Quality (average)
	Node Quantity	Element Quantity	
Base Piston	316197	208595	0.82
0.2 mm Coated	355475	215467	0.79
0.4 mm Coated	370882	219597	0.78
0.6 mm Coated	385398	223087	0.77
0.8 mm Coated	399914	226577	0.76

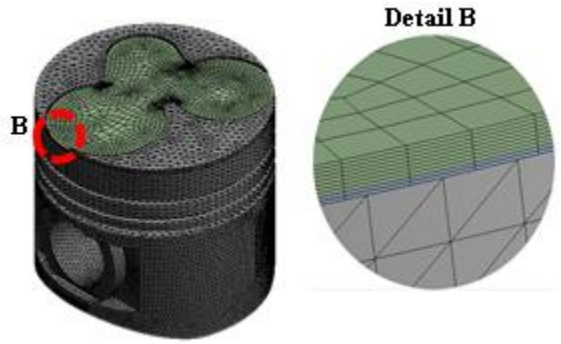

Figure 2. *Meshed model of 0.2 mm NiCrAl 0.8 mm ZrO_2*

SOLID87 3-D 10-Node Tetrahedral Thermal Solid and SOLID90 3-D 20-Node Thermal Solid used as element types for meshing the volumes.

SOLID87 is well suited to model irregular meshes (such as produced from various CAD/CAM systems). The element has one degree of freedom, temperature, at each node. SOLID90 has 20 nodes with a single degree of freedom, temperature, at each node. The 20-node elements have compatible temperature shapes and are well suited to model curved boundaries [18].

After creating the mesh, material properties of the piston, binding layer and thermal coat was defined. Table 2 also shows the materials and their thermal properties used at finite element analyses.

Table 2. *Thermal properties of the materials*

Material	Thermal conductivity [W/m °C]	Thermal expansion 10−6 [1/°C]	Specific heat [J/kg °C]
AlSi	237.5	21	960
NiCrAl	16.1	12	764
ZrO_2	3	11	460

The next step of the analysis is defining the boundary conditions. For this mathematical model different boundary conditions were defined in seven regions [19]. Boundary conditions are listed below at Figure 3 and Table 3 below. After creating the mesh, defining material properties and boundary conditions, solutions were made for five different models.

Table 3. *Properties of boundary conditions*

Region	Film Coefficient $W/mm^{2}{}^{\circ}C$	Ambient Temperature $^{\circ}C$
A	$8x10^{-4}$	650
B	$2.3x10^{-4}$	300
C	$6.25x10^{-4}$	85
D	$1.15x10^{-4}$	110
E	$1.91x10^{-4}$	110
F	$7.17x10^{-4}$	110
G	$625x10^{-4}$	85

3. Results of the Analysis

As previously mentioned, five different models were used for the solution. First is original piston without coat. The other four models are coated. The binder coating on all models is 0.2 mm. Thermal coatings of four models are 0.2,0.4,0.6 and 0.8 mm ZrO_2. All models were solved under the same boundary conditions. Finally, the responses of the models to the same boundary conditions were compared. Solutions were made in a computer with four core Intel Pentium I7-3770K @3.50 Hz and 16 Gb physical memory on windows 10 x64 platform. To compare the results, 4 paths were formed on the piston combustion chamber surface, 5 mm below the piston combustion chamber, above the binding coating and above the thermal coating. Detail of this path can be seen at figure 1(H). Likewise, the heat flux of all models is compared. Figure 4,5,6,7 shows temperature effect (TE) of termal barrier coating (TBC) on paths named H and temperature distrubition (TD) on several surfaces. Further, total heat flux of uncoated and 0.8 mm ZrO_2 coated pistons can be seen Figure 8. After solutions for each coating, results were examined according to the upper surface of the combustion chamber of the uncoated piston. Maximum temperature occured 242.3 $^{\circ}C$ at uncoated piston, 236.7 $^{\circ}C$ at 0.2 mm ZrO_2 coated piston, 232.2 $^{\circ}C$ at 0.4 mm ZrO_2 coated piston, 227.95 $^{\circ}C$ at 0.6 mm ZrO_2 coated piston and 224.7 $^{\circ}C$ at 0.8 mm ZrO_2 coated piston. All results can be seen at Table 4.

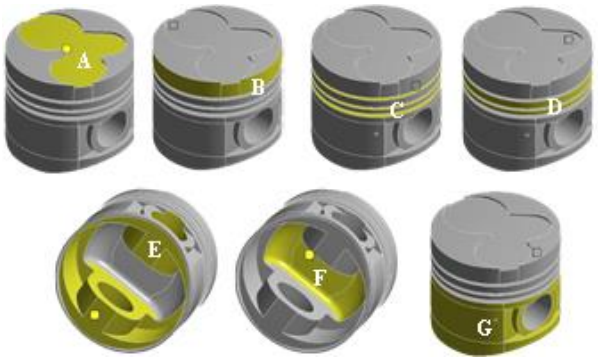

Figure 3. *Boundary condition regions of the piston*

Table 4. *Results of the finite element analysis*

Type	Uncoated	0.2 mm coated	0.4 mm coated	0.6 mm coated	0.8 mm coated
Combustion chamber top surface max. temp.	242.3	236.68	232.16	227.95	224.70
Binding layer top surface max. temp.	---	250.31	245.16	240.44	225.32
Thermal coating top surface max. temp.	---	264.97	277.79	290.67	299.38
Heat flux max	0.83	1	0.95	1.22	1.44
Piston Section max. temp.	236.4	230.63	226.27	222.27	219.31

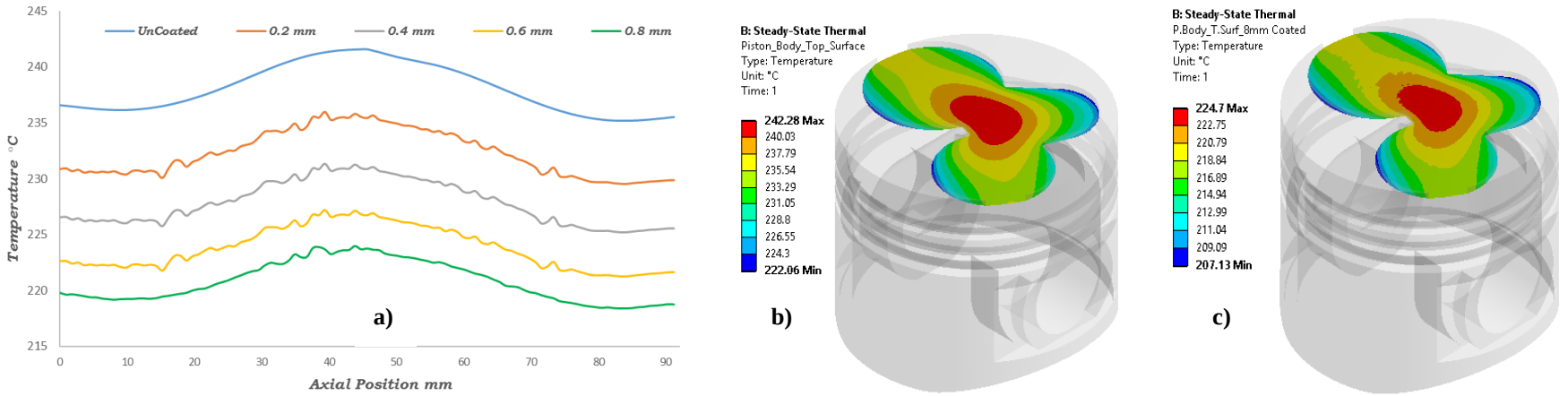

Figure 4. *TE of TBC on piston combustion chamber top surface changing with distance (a), TD on combustion chamber of uncoated piston (b), TD on combustion chamber of uncoated piston with 0.8 mm ZrO_2 coated (c).*

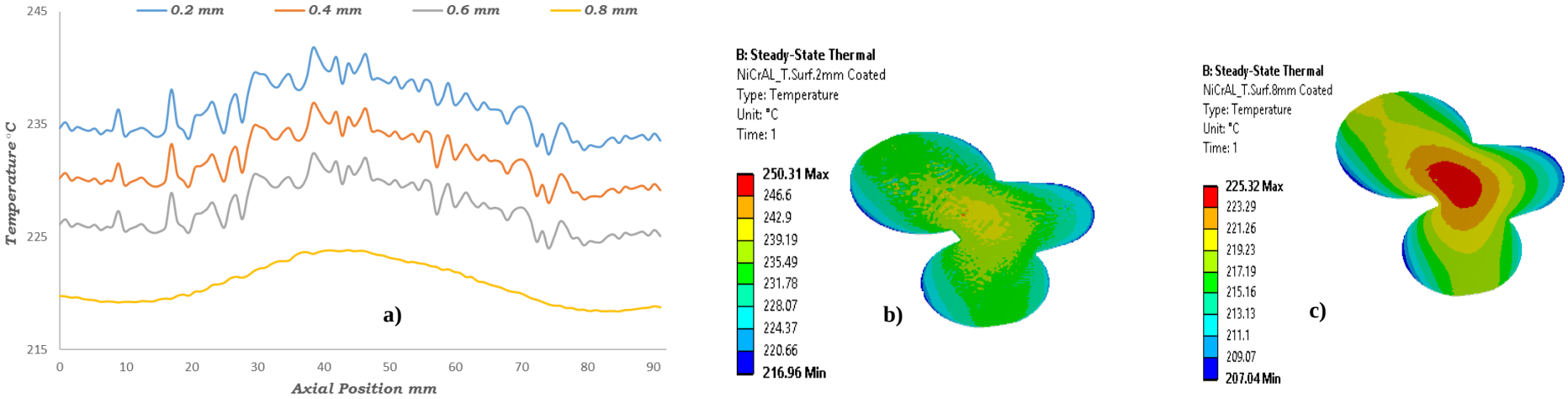

Figure 5. *TE of TBC on Binding_Layer_Top_Surface changing with distance (a), TD on 0.2 mm NiCrAl coat with 0.2 mm ZrO_2 coated (b), TD on 0.2 mm NiCrAl coat with 0.8 mm ZrO_2 coated (c).*

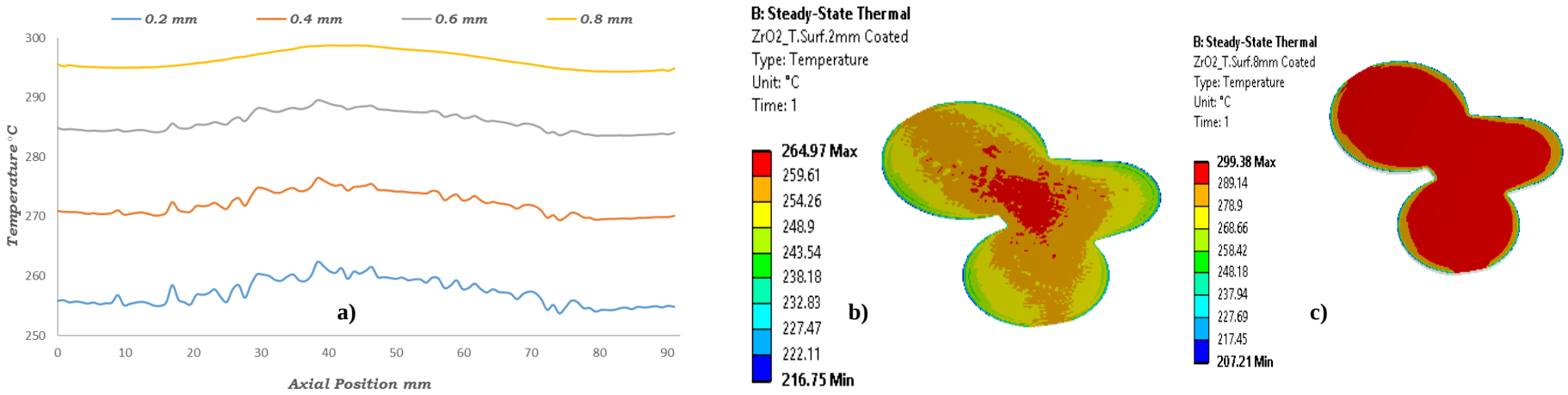

Figure 6. *TE of TBC on Thermal_Coating_Top_Surface changing with distance (a), TD on 0.2 mm ZrO_2 coated (b), TD on 0.8 mm ZrO_2 coated (c).*

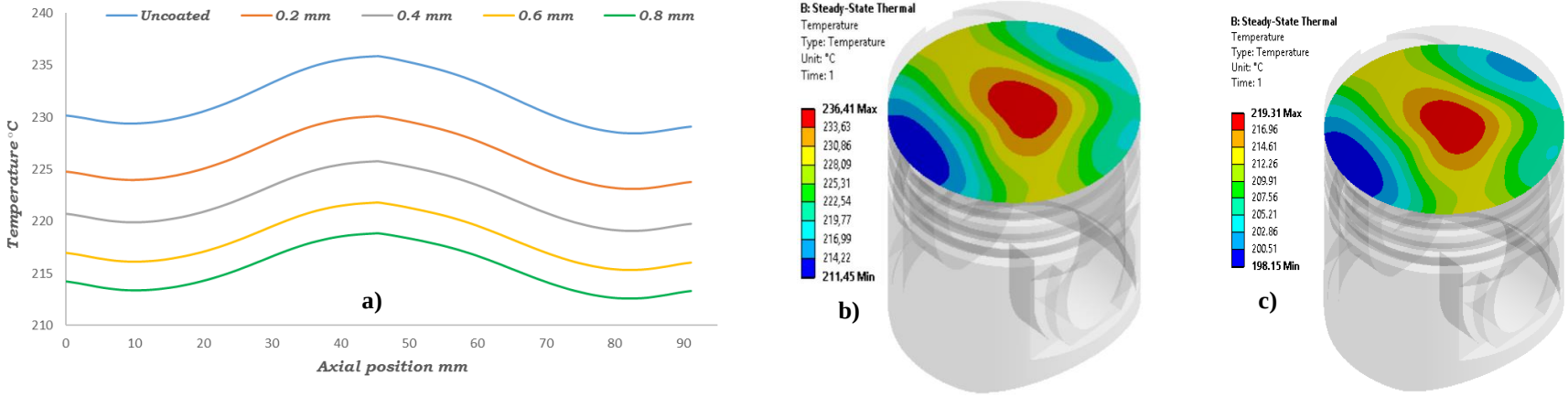

Figure 7. *TE of TBC on 5mm below combustion chamber changing with distance (a),TD on 5 mm below combustion chamber at uncoated piston(b), TD on 5 mm below combustion chamber at coated with 0.8 mm ZrO_2 (c).*

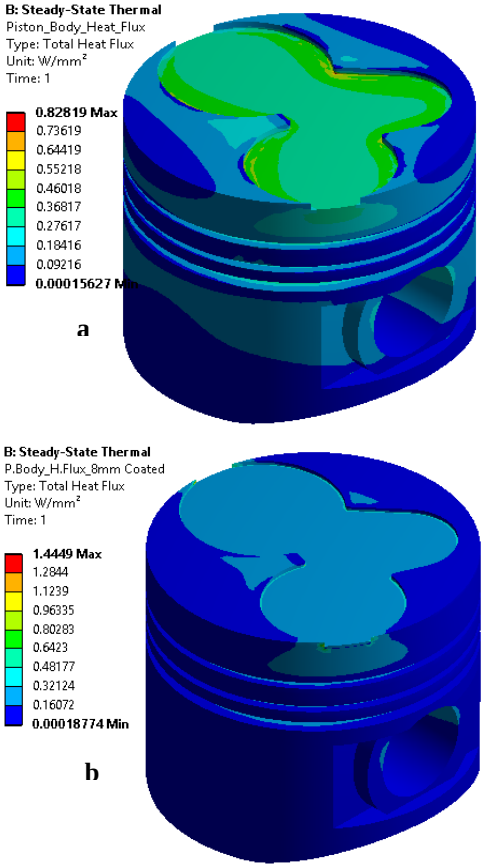

Figure 8. *Total heat flux of uncoated piston a) and total heat flux of 0.8 mm ZrO_2 coated piston.*

4. Conclusion

When the results were examined, in the terms of occurring maximum temperature at piston combustion chamber top surface level (Figure 4), it was observed that there was 7% decrease between the uncoated piston and 0.8 mm ZrO_2 coated piston. Looking at the results of the bond coat (binding layer), a temperature decrease of 10% is observed (Figure 5). The temperature increase as a value of 13 % is observed on the top surface of the thermal coating (Figure 6).
This means that, the temperature is more confined on the thermal coating surface depending on the coating increasing.

At piston section level (5 mm below the combustion chamber top surface of uncoated piston, Figure 7) , a 7 % temperature decrease seen. At the end of the study, as expected a reduction in temperature was achieved by the coating of combustion chamber top surface. The next step of this study is optimization of the binding and thermal coats. Also make an experimental study in terms of verify the results.

References

[1] Fu, Y., Shao, C., Cai, C., Wang, Y., Zhou, Y., Zhou, G., Temperature induced structure degradation of yttria-stabilized zirconia thermal barrier coatings, Surface & Coatings Technology 351 (2018), 21–28 https://doi.org/10.1016/j.surfcoat.2018.07.057

[2] Khan, M., Zeng, Y., Lan, Z., Wang, Y., Reduced thermal conductivity of solid solution of 20% CeO_2 +ZrO_2 and 8% Y_2O_3 +ZrO_2 prepared by atmospheric plasma spray technique, Ceramics International, https://doi.org/10.1016/j.ceramint.2018.09.252

[3] Liu, H., Cai, J., Zhu, J., CMAS (CaO–MgO–Al_2O_3–SiO_2) resistance of Y_2O_3-stabilized ZrO_2 thermal barrier coatings with Pt layers, Ceramics International 44 (2018), 452–458 https://doi.org/10.1016/j.ceramint.2017.09.197

[4] Wang, J., Sun, J., Jing, Q., Liu, B., Zhang, H., Yu, Y., Yuan, J., Dong, S., Zhou, X., Cao, X., Phase stability and thermo-physical properties of ZrO2-CeO2-TiO2 ceramics for thermal barrier coatings, Journal of the European Ceramic Society 38 (2018), 2841–2850, https://doi.org/10.1016/j.jeurceramsoc.2018.02.019

[5] Ramaswamy, P., Shankar V, Reghu V.R., Mathew, N., Manoj, K.S., A Model to Predict the Influence of Inconsistencies in Thermal Barrier Coating (TBC) Thicknesses in Pistons of IC Engines, Materials Today: Proceedings 5 (2018), 12623–12631 https://doi.org/10.1016/j.matpr.2018.02.245

[6]Dudareva, N.Y., Enikeev, R.D.a, Ivanov, V.Y., Thermal Protection of Internal Combustion Engines Pistons, Procedia Engineering 206 (2017) 1382–1387 https://doi.org/10.1016/j.proeng.2017.10.649

[7]Bolek, T., Sitek, R., Sienkiewicz, J., Dobosz, R., Mizera, J., Kobayashi, A., Kurzydlowski, K.J., Simulation of the influence of the interface roughness on the residual stresses induced in (ZrO_2+Y_2O_3)+NiAl-type composite coatings deposited on Inconel 713C, Vacuum 136 (2017), 221-228 https://doi.org/10.1016/j.vacuum.2016.11.003

[8] Kumar, P.S.R., Kumar, P.N., Janardhana, G.R., Static Analysis of Al - ZrO_2FG Thick Plate Using Graded FEM, Materials Today: Proceedings 4 (2017), 8117–8126 https://doi.org/10.1016/j.matpr.2017.07.152

[9] Yerrennagoudaru, H., Manjunatha, K., Combustion analysis of modified inverted “M” type piston for diesel engine with platinum coating and without coating by using CFD, Materials Today: Proceedings 4 (2017), 2333–2340 https://doi.org/10.1016/j.matpr.2017.02.082

[10] Ma, G., Yan, S., Wu, D., Miao, Q., Liu, M., Niu, F., Microstructure evolution and mechanical properties of ultrasonic assisted laser clad yttria stabilized zirconia coating, Ceramics International 43 (2017), 9622–9629 https://doi.org/10.1016/j.ceramint.2017.04.103

[11] Kocabicak, U., Mimaroglu, A., Sarikaya, O., Mete, O.H., Comparison of the developed thermal stresses in Al_2O_3-SG, ZrO_2-12%Si+Al and ZrO_2-SG coating systems subjected to thermal loading, Materials and Design 20 (1999), 287-290 https://doi.org/10.1016/S0261-3069(99)00041-2

[12] Celik, E., Sarikaya, O., The effect on residual stresses of porosity in plasma sprayed MgO–ZrO2 coatings for an internal combustion diesel engine, Materials Science and Engineering A 379 (2004), 11–16 https://doi.org/10.1016/j.msea.2003.12.019

[13] Taymaz, I., Mimaroglu, A., Avci, E., Ucar, V., Gur, M., Comparison of thermal stresses developed in Al_2O_3–SG, ZrO_2–(12% Si+Al) and ZrO_2–SG thermal barrier coating systems with NiAl, NiCrAlY and NiCoCrAlY interlayer materials subjected to thermal loading,Surface and Coatings Technology 116–119 (1999), 690–693 https://doi.org/10.1016/S0257-8972(99)00121-8

[14] Sarikaya, O., Celik, E., Effects of residual stress on thickness and interlayer of thermal barrier ceramic MgO–ZrO_2 coatings on Ni and AlSi substrates using finite element method, Materials and Design 23 (2002), 645–650 https://doi.org/10.1016/S0261-3069(02)00047-X

[15] Mimaroglu, Kocabicak, U., A., Genc, S., Influence of porosity characteristics in Mg0.ZrO_2-GG coating subjected to thermal loading, Materials & Design, 18(1997), 77-80 https://doi.org/10.1016/S0261-3069(97)00042-3

[16] Khor, K.A., Gu, Y.W., Effects of residual stress on the performance of plasma sprayed functionally graded ZrO_2/NiCoCrAlY coatings, Materials Science and Engineering A277 (2000), 64–76 https://doi.org/10.1016/S0921-5093(99)00565-1

[17] Mimaroglu, A., Yenihayat, O.F. Avci, E., Numerical analysis of fracture in ceramic coatings subjected to thermal loading, Materials&Design 17 (1996), 283-287 https://doi.org/10.1016/S0261-3069(97)00023-X

[18] ANSYS Workbench Help

[19] Buyukkaya, E., Thermal analysis of functionally graded coating AlSi alloy and steel pistons, Surface & Coatings Technology 202 (2008) 3856–3865 https://doi.org/10.1016/j.surfcoat.2008.01.034